DATA-DRIVEN MODELS FOR CANOPY TEMPERATURE-BASED IRRIGATION SCHEDULING

B. A. King, K. C. Shellie, D. D. Tarkalson, A. D. Levin, V. Sharma, D. L. Bjorneberg

Beyond 2020, VISION OF THE FUTURE
Collection
Research

HIGHLIGHTS

- Artificial neural network modeling was used to predict crop water stress index lower reference canopy temperature.
- Root mean square error of predicted lower reference temperatures was <1.1°C for sugarbeet and Pinot noir wine grape.
- Energy balance model was used to dynamically predict crop water stress index upper reference canopy temperature.
- Crop water stress index for sugarbeet was well correlated with irrigation and soil water status.
- Crop water stress index was well correlated with midday leaf water potential of wine grape.

ABSTRACT. *Normalized crop canopy temperature, termed crop water stress index (CWSI), was proposed over 40 years ago as an irrigation management tool but has experienced limited adoption in production agriculture. Development of generalized crop-specific upper and lower reference temperatures is critical for implementation of CWSI-based irrigation scheduling. The objective of this study was to develop and evaluate data-driven models for predicting the reference canopy temperatures needed to compute CWSI for sugarbeet and wine grape. Reference canopy temperatures for sugarbeet and wine grape were predicted using machine learning and regression models developed from measured canopy temperatures of sugarbeet, grown in Idaho and Wyoming, and wine grape, grown in Idaho and Oregon, over five years under full and severe deficit irrigation. Lower reference temperatures (T_{LL}) were estimated using neural network models with Nash-Sutcliffe model efficiencies exceeding 0.88 and root mean square error less than 1.1°C. The relationship between T_{LL} minus ambient air temperature and vapor pressure deficit was represented with a linear model that maximized the regression coefficient rather than minimized the sum of squared error. The linear models were used to estimate upper reference temperatures that were nearly double the values reported in previous studies. A daily CWSI, calculated as the average of 15 min CWSI values between 13:00 and 16:00 MDT for sugarbeet and between 13:00 and 15:00 local time for wine grape, were well correlated with irrigation events and amounts. There was a significant ($p < 0.001$) linear relationship between the daily CWSI and midday leaf water potential of Malbec and Syrah wine grapes, with an R^2 of 0.53. The data-driven models developed in this study to estimate reference temperatures enable automated calculation of the CWSI for effective assessment of crop water stress. However, measurements taken under conditions of wet canopy or low solar radiation should be disregarded as they can result in irrational values of the CWSI.*

Keywords. *Canopy temperature, Crop water stress index, Irrigation scheduling, Leaf water potential, Sugarbeet, Wine grape.*

Submitted for review in January 2020 as manuscript number NRES 13901; approved for publication as a Research Article and as part of the National Irrigation Symposium 2020 Collection by the Natural Resources & Environmental Systems of ASABE in May 2020.

Mention of company or trade names is for description only and does not imply endorsement by the USDA. The USDA is an equal opportunity provider and employer.

The authors are **Bradley A. King,** Research Agricultural Engineer, USDA-ARS Northwest Irrigation and Soils Research Laboratory, Kimberly, Idaho; **Krista C. Shellie,** Research Horticulturalist (retired), USDA-ARS Horticultural Crops Research Unit, Corvallis, Oregon; **David D. Tarkalson,** Research Agronomist, USDA-ARS Northwest Irrigation and Soil Research Laboratory, Kimberly, Idaho; **Alexander D. Levin,** Viticulturist and Assistant Professor, Oregon State University Southern Oregon Research and Extension Center, Central Point, Oregon; **Vivek Sharma,** Assistant Professor, Department of Agricultural and Biological Engineering, University of Florida, Gainesville, Florida; **David L. Bjorneberg,** Research Leader, USDA-ARS Northwest Irrigation and Soils Research Laboratory. **Corresponding author:** Bradley A. King, USDA-ARS NWISRL, 3793 North 3600 East, Kimberly, ID 83341; phone: 208-423-6501; e-mail: brad.king@usda.gov.

Two key elements for effective irrigation water management (i.e., irrigation scheduling) are optimum timing of water application and applying an amount of water that replaces crop evapotranspiration (ET). Conventional soil water balance-based irrigation scheduling relies on tracking estimated crop ET, maintaining a continual numerical soil water balance, and irrigating when available soil water is forecasted to reach a predetermined lower limit based on crop characteristics, known soil water holding capacity, and known effective crop root zone depth. Often, soil water holding capacity and crop root zone depth are unknown and estimated. Soil water content monitoring is necessary to periodically validate or adjust the numerical soil water balance to minimize calculation errors introduced by the use of generalized ET crop coefficients and estimated and variable water application inefficiency (Ashley et al., 1996; Jones, 2004; Melvin and Yonts, 2009; Werner, 1993).

Irrigation scheduling can also be based on frequent or continuous soil water monitoring alone and irrigating when a predetermined lower limit is approached to fully or partially replace soil water depletion, eliminating the need for maintaining a numerical soil water balance (Hansen et al., 2007; Irmak et al., 2016; Vellidis et al., 2008).

Soil water monitoring can be achieved using a variety of techniques, with various tradeoffs among them. Regardless of the selected technique, there will be a cost for the equipment, labor for installation, maintenance, and removal, and a cost in terms of the time required for the irrigation manager to interpret the data. Ultimately, the manager needs a fundamental knowledge of soil-water-plant relationships to transform soil water content data into an effective irrigation scheduling decision, e.g., conversion of volumetric soil water content values into available soil water based on site-specific soil-water characteristics, crop effective rooting depth, and critical soil water availability threshold of the crop. Most soil water measurement techniques have small sampling volumes (Muñoz-Carpena, 2004). The relatively small sampling volumes of soil water measurement techniques require that multiple soil water sampling sites are needed to reliably quantify soil water content at the field scale for irrigation scheduling (Li et al., 2020; Zotarelli, 2013), but equipment and labor costs limit the number of measurement sites in practice. In drip-irrigated horticultural crops such as wine grapes, root zone soil water content is three-dimensional (Davenport et al., 2008), which makes sensor placement for quantifying soil water content important. For example, Williams and Trout (2005) reported that nine neutron probe measurements in one root zone quadrant to a depth of 3 m were necessary to quantify soil water content of drip-irrigated grape vines.

Many features of a plant's physiology respond directly to changes in water status in the plant tissues rather than to changes in the bulk soil water availability (Jones, 2004). Plant canopy temperature increases when solar radiation is absorbed and cools when water is evaporated (transpiration) within the leaf structure. A water-stressed plant canopy will have reduced transpiration and a higher temperature than a non-stressed canopy (Raschke, 1960; Tanner, 1963). Infrared radiometers have been used to measure plant canopy temperature under field conditions to estimate ET and drought stress in many crops (Hatfield, 1983; Jackson et al., 1981; Idso et al., 1981; Maes and Steppe, 2012). Infrared thermometry is nondestructive, can be measured continuously, can be mounted on mobile platforms for spatial and temporal monitoring (Sadler et al., 2002; Nayak, 2005), and can be less expensive (Mahan and Yeater, 2008) than soil water sensing. Plant canopy temperature can be influenced by abiotic factors other than soil water availability as well as biotic factors such as disease (DeJonge et al., 2015), which can lead to elevated canopy temperature and potential error in irrigation scheduling from incorrect interpretation of the elevated canopy temperature. A wet canopy and/or low solar radiation masks the link between soil water availability and canopy temperature, precluding appropriate irrigation scheduling when the canopy is wet from irrigation or rainfall or cloudy conditions (Jones 1999, 2004; Bockhold et al., 2011). Thus, canopy temperature measurement for irrigation scheduling is likely best suited for arid climates (Jones 1999). Despite more than 40 years of canopy temperature-based irrigation scheduling research, continued effort is needed to fully develop canopy measurement into a commercially viable irrigation scheduling technique (Lo, 2018).

Canopy temperature measurement for irrigation scheduling articulated as a simple empirical relationship, called the crop water stress index (CWSI), was proposed nearly 40 years ago by Idso et al. (1981) and Jackson et al. (1981). The CWSI is a simple linear scale ranging from 0 when, under identical climatic conditions, the measured canopy temperature (T_c) is equal to the well-watered canopy temperature (T_{LL}) and 1 when T_c is equal to the non-transpiring canopy temperature (T_{UL}). Canopy temperatures T_{LL} and T_{UL} are respectively the lower and upper reference temperatures used to normalize the 0 to 1 range of the CWSI. Normalizing is used to account for the effects of atmospheric conditions, including air temperature (T_a), relative humidity (RH), solar radiation (R_s), and wind speed (WS), on transpiration and canopy temperature. However, practical application of the CWSI has been limited by the difficulty of estimating T_{LL} and T_{UL} (Maes and Steppe, 2012). Theoretical determination of crop-specific constants for T_{LL} and T_{UL} relative to ambient air temperature has not been fruitful due to the poorly understood and complex influences of canopy architecture and environmental conditions on the soil-plant-air continuum (Idso et al., 1981; Jones, 1999, 2004; Payero and Irmak, 2006). In the original development and application of the CWSI concept, T_{LL} and T_{UL} were experimentally determined from field measurements with $T_{LL} - T_a$ linearly correlated with vapor pressure deficit (VPD) to account for major climatic effects confounding T_c measurements (Idso, 1982). In the initial development and application of CWSI, canopy temperature measurements were restricted to times near solar noon on cloudless days to limit the effect of variable solar radiation on canopy temperature and stomatal conductance. Ideally, in application of the CWSI, companion plots of the crop under well-watered and non-transpiring conditions would be available for direct measurement of T_{LL} and T_{UL}. In commercial agriculture, use of companion plots is not feasible, nor is it possible to maintain a crop canopy under non-transpiring conditions. Alternative methods of estimating T_{LL} and T_{UL} are needed and have been investigated. In research studies, artificial wet and dry reference surfaces have been used successfully to estimate T_{LL} and T_{UL} (Alchanatis et al., 2010; Cohen et al., 2005; Jones, 1999; Jones et al., 2002; Leinonen and Jones, 2004; O'Shaughnessy et al., 2011; Pou et al., 2014); however, the required maintenance of the artificial surfaces limits their potential use for maintenance-free automation in commercial crop production.

Physical models have been developed to estimate T_{LL} and T_{UL} with varying degrees of success (Jones, 1992) and often require ancillary measurements to reliably estimate equation parameters. Jackson et al. (1981) proposed an energy balance equation for $T_c - T_a$ at the plant-atmosphere interface as:

$$T_c - T_a = \frac{r_a R_n}{\rho c_p} \frac{\gamma\left(1+\frac{r_c}{r_a}\right)}{\Delta+\gamma\left(1+\frac{r_c}{r_a}\right)} - \frac{e_s - e_a}{\Delta+\gamma\left(1+\frac{r_c}{r_a}\right)} \quad (1)$$

where

r_a = aerodynamic resistance (s m^{-1})

R_n = net radiation (W m^{-2})

ρ = density of air (kg m^{-3})

c_p = heat capacity of air (J kg^{-1} °C^{-1})

γ = psychrometric constant (Pa °C^{-1})

Δ = slope of the water saturation vapor pressure and air temperature relationship (Pa °C^{-1})

r_c = canopy resistance (s m^{-1})

e_s = water saturation vapor pressure (kPa) at T_a

e_a = actual water vapor pressure (kPa) of the air.

Jackson et al. (1981) also discussed the influence of plant and atmospheric conditions on $T_c - T_a$, proposing that the upper limit to canopy temperature can be expressed as:

$$T_{UL} - T_a = \frac{r_a R_n}{\rho c_p} \tag{2}$$

because r_c (eq. 1) of a non-transpiring canopy can be assumed to increase without limit ($r_c \rightarrow \infty$) in practice. The relationship between $T_c - T_a$ and $e_s - e_a$ (eq. 1) of well-watered crops in arid climates is often found to be linear (Idso, 1982). Based on this observation, O'Toole and Real (1986) proposed formulating equation 1 as a linear function of VPD:

$$T_c - T_a = a + b\left(e_a - e_s\right) \tag{3}$$

where a and b are the intercept and slope regression coefficients, respectively. Theoretically, estimation of the regression coefficients requires variables other than T_c, T_a, e_s, and e_a to be held constant, which is impossible under field conditions. O'Toole and Real (1986) reasoned that using values averaged over the duration of canopy temperature measurement for the remaining variables in equation 1 provided a practical means for estimating the regression coefficients in equation 3. Equating equations 1 and 3 and solving for the average canopy resistance ($\overline{r}_{cp}$) and average aerodynamic resistance ($\overline{r}_{ap}$) for well-watered conditions resulted in:

$$\overline{r}_{ap} = \frac{\overline{\rho} c_p a}{\overline{R}_n b\left(\overline{\Delta} + 1/b\right)} \tag{4}$$

$$\overline{r}_{cp} = -\overline{r}_{ap}\left[\frac{\overline{\Delta} + 1/b}{\overline{\gamma}} + 1\right] \tag{5}$$

where $\overline{R}_n$ is the average R_n, $\overline{\Delta}$ is the average Δ, and $\overline{\rho}$ is the average ρ of the dataset used to determine a and b in equation 3. Substituting $\overline{r}_{ap}$ for r_a and $\overline{R}_n$ for R_n with measured T_a in equation 2 allows estimation of T_{UL}. This physical approach to estimating T_{UL} does not require additional crop physical measurements other than well-watered canopy temperature and common meteorological measurements. Han et al. (2018) used this approach of estimating T_{UL} to compute a CWSI-adjusted soil water balance for water-stressed maize with good results.

Various data-driven empirical methods have been used to estimate T_{LL} and T_{UL} since the introduction of the CWSI concept. Payero and Irmak (2006) used multiple linear regression (MLR) with independent variables T_a, R_s, crop height, WS, and VPD or RH to predict the canopy temperature of well-watered corn and soybean with coefficients of determination (R^2) of 0.69 to 0.84 between the predicted and measured canopy temperatures. For water-stressed corn, Irmak et al. (2000) determined that T_{UL} was 4.6°C to 5.1°C above air temperature. In several subsequent studies with crops other than corn, a value of air temperature plus 5.0°C has been used for T_{UL} (Alchanatis et al., 2010; Cohen et al., 2005; Möller et al., 2007). O'Shaughnessy et al. (2011) used maximum daily air temperature plus 5.0°C for T_{UL} of soybean and cotton. King and Shellie (2016) also obtained good results in estimating T_{LL} using MLR for wine grapes. They used T_a + 15°C for T_{UL} based on the cumulative distribution of maximum measured daily $T_c - T_a$ of deficit-irrigated wine grapes. Regression, by necessity, simplifies complex, unknown interactions into *a priori* or assumed multiple linear or nonlinear relationships (Payero and Irmak, 2006). King and Shellie (2016) also evaluated the use of artificial neural network (NN) models for estimating T_{LL} of wine grape with better results than MLR. Artificial NNs have been used successfully to model complex, unknown relationships and predict physical conditions, such as ET (Bhakar et al., 2006; Kumar et al., 2002; Trajkovic et al., 2003), irrigation scheduling (Karasekreter et al., 2012), and many other water resource applications (ASCE, 2000).

A major obstacle to wide spread adoption of the CWSI concept in irrigated agriculture is the lack of regionally generalized or crop-specific relationships for T_{LL} and T_{UL}. Over the past 40 years, numerous research studies have collected field data and used linear regression to model the relationship between $T_c - T_a$ and VPD for numerous crops. All data-driven models are specific to the dataset used to quantify the relationship between $T_c - T_a$ and VPD and are by nature location, climate, and year specific, limiting transferability to other locations. In the absence of solved physical models for T_{LL} and T_{UL}, the only recourse is to continue to develop crop-specific generalized data-driven models. This will require an extensive database of T_c and associated climatic variables for a specific crop spanning a region over several years. The objective of the research summarized in this article was to develop and evaluate general data-driven models for T_{LL} and T_{UL} for sugarbeet and wine grape in the irrigated northwestern region of the U.S. The responses of daily CWSI values, calculated using estimated values for T_{LL} and T_{UL}, to irrigation events were compared to that of measured available soil water for sugarbeet and plant water potential for wine grape to evaluate the performance of the data-driven models.

Materials and Methods

Sugarbeet

Study plots of sugarbeet were gown at the USDA-ARS Northwest Irrigation and Soils Research Laboratory (NWISRL) near Kimberly, Idaho, in 2014 to 2019 and at the University of Wyoming Powell Research and Extension

Center (PREC) near Powell, Wyoming, in 2018. A randomized block experimental design was used at each location. Four irrigation treatments with four replicates were evaluated at NWISRL, consisting of fully irrigated (FIT), 75% FIT, 50% FIT, and 25% FIT. The FIT represented the condition in which the crop was irrigated two or three times a week with a cumulative depth equal to weekly cumulative estimated ET. Three irrigation treatments with three replicates were evaluated at PREC, consisting of FIT, 75% FIT, and 60% FIT. Production practices on the experimental plots followed local commercial practices. Estimated crop ET at NWISRL was based on the 1982 Kimberly-Penman alfalfa reference ET model and daily crop coefficients (Wright, 1982) obtained from an Agrimet (U.S Bureau of Reclamation, https://www.usbr.gov/pn/agrimet/) weather station located within 4.5 km of the study site. Estimated crop ET at PREC was based on the ASCE standardized reference ET equation (ASCE, 2005) and daily crop coefficients (Wright, 1982) using daily climatic data from an on-site weather station (Sharma et al., 2018). Irrigation was applied using sprinkler irrigation from either lateral-move irrigation systems or solid set micro sprinkler system. The soil at NWISRL was a Portneuf silt loam (coarse-silty mixed mesic Durixerollic Calciorthid) classified as very deep and well drained with weak silica cementation ranging from 30 to 45 cm deep that may restrict root growth (USDA, 1998). The soil at PREC was a Garland loam (fine-loamy over sandy or sandy-skeletal, mixed, superactive, mesic Typic Haplargids) that consisted of loam changing to extremely gravelly loamy sand below 0.8 m that hinders soil sampling, with a restrictive layer beyond 2.0 m (USDA, 2019). Soil water content was measured periodically throughout the growing season using neutron probes to a depth of 2.2 m in 0.15 m depth increments at NWISRL and to a depth of 1 m in 0.3 m increments at PREC. Additionally, at NWISRL, soil water content of the 0 to 0.15 m soil depth was measured at 30 min intervals using time domain reflectometery (TDR 100, Campbell Scientific, Logan, Utah) with two probes in the center crop row of a treatment plot.

Canopy temperature was measured at both research locations using infrared radiometers (SI-121, Apogee Instruments, Logan, Utah) with a 36° field of view. One radiometer was used in each of two replicates of each irrigation treatment (eight total) at NWISRL in 2014, 2015, and 2016, and one radiometer was used in each replication of the irrigation treatments (16 total) in subsequent years. Two paired sensors were used in two replications of the irrigation treatments (12 total) at PREC. The infrared radiometers were positioned approximately 0.6 m above the canopy and oriented northeasterly approximately 45° from nadir with the sensor view aimed at the sunlit canopy surface. The infrared radiometers were installed when the sugarbeet crop neared full cover, usually in the first or second week of July. Climatic parameters R_s (SP-110 pyranometer, Apogee Instruments), T_a, RH (HMP50 temperature and humidity probe, Campbell Scientific), and WS (034B, Met One Instruments, Grants Pass, Ore.) were measured at both locations. Canopy temperature and climatic parameters were measured every minute with a datalogger (CR1000 or CR6, Campbell Scientific) and recorded as 15 min averages. The equipment was removed at harvest, usually mid to late September.

Wine Grape

Study plots of wine grape were grown at the University of Idaho Parma Research and Extension Center (UIPREC) near Parma, Idaho, from 2013 to 2017 and at a commercial vineyard near Wilderville, Oregon, in 2018 and 2019. Several wine grape (*Vitis vinifera* L.) cultivars were studied at UIPREC, but only results for Malbec, Syrah, and Pinot noir are included in this article. Pinot noir was the only wine grape cultivar studied at the Oregon site. Row by vine spacing was 2.4 m × 1.8 m at UIPREC and 2.4 m × 1.2 m at the Oregon site. At UIPREC, the vines were grown with double trunks on a vertically shoot positioned (VSP), two-wire trellis system with moveable catch wires. The vines were trained to bilateral cordons and spur-pruned annually to 16 buds m^{-1} of cordon. In Oregon, the vines were trained and pruned similarly but were trained with single trunks. Irrigation at both sites was applied using drip irrigation tubing suspended about 30 cm above ground in the vine row. Disease and pest control and hedging were managed according to local commercial practices. Alley and vine rows were maintained free of vegetation at UIPREC and mowed at the Oregon site. The experimental design at both locations was a randomized block with five replicates. Alfalfa and grass reference crop ET were obtained from an Agrimet (U.S Bureau of Reclamation, https://www.usbr.gov/pn/agrimet/) weather station located within 4.5 km of the UIPREC study site and 50 km from the Oregon study site. A local industry-developed crop coefficient curve was used at UIPREC (King and Shellie, 2016), while row-spacing-adjusted crop coefficients (Williams, 2014) for VSP trellises were used at the Oregon site. Vine water stress was monitored weekly between fruit set and harvest using leaf water potential (LWP) at UIPREC and stem water potential (SWP) at the Oregon site. Irrigation treatments were FIT, 70% FIT, and 35% FIT at UPREC and FIT, 25% FIT, and LD25 at the Oregon site. The LD25 treatment was irrigated at 100% estimated crop ET (ET_c) from irrigation initiation to the onset of ripening (veraison) and then at 25% of ET_c from veraison to harvest. In Oregon, irrigation was initiated when a plot-averaged threshold SWP value of -0.8 MPa was reached. After irrigation initiation, the vines were irrigated two or three times per week until just prior to harvest (late September). Measurements of SWP were collected using a pressure chamber (model 615, PMS Instruments, Albany, Ore.) as described by Levin (2019). Measurements of SWP were collected in each treatment plot near solar noon on fully expanded, sunlit leaves, with bags left on leaves for minimum of 10 min. The same operator and instrument combination was used for all measurement dates. Measurements of LWP at UIPREC were collected near solar noon on two fully expanded, sunlit leaves per treatment plot using a pressure chamber (model 610, PMS Instruments) as described by Shellie (2006).

Canopy temperatures at both wine grape study sites were measured using the same infrared radiometer types as described for sugarbeet. The radiometers were positioned ap-

proximately 15 to 30 cm above fully expanded leaves located at the top of the vine canopy and pointed northeasterly at approximately 45° from nadir, with the sensor view aimed at the center of solar noon sunlit leaves. The measured canopy area received full sunlight exposure during midday. The temperature sensing area was approximately 10 to 20 cm in diameter. The possibility of bare soil visibility in the background was limited by leaf layers within the canopy below the measured canopy location. The infrared radiometer sensor view was periodically checked and adjusted as necessary to ensure that the field of view concentrated on sunlit leaves near the top of the canopy. The infrared radiometers were installed after fruit set, usually mid to late June. Two paired radiometers were used in FIT treatment plots and one radiometer was used in three replicates of the 70% FIT and 35% FIT treatments at UIPREC (18 total). One radiometer was used in three replicates of each irrigation treatment (nine total) at the Oregon site. Climatic parameters R_s, T_a, RH, and WS were measured at both locations using the same sensor types as described for sugarbeet. Canopy temperature and climatic parameters were measured every minute with a datalogger (CR1000 or CR6, Campbell Scientific) and recorded as 15 min averages. The equipment was removed prior to harvest, usually mid to late September.

MODELING T_{LL} AND T_{UL}

Non-water stressed canopy temperature (T_{LL}) for sugarbeet and for each wine grape cultivar was predicted as a function of climatic conditions (R_s, T_a, RH, and WS) using multilayer perceptron feed-forward NN models developed from a database of measured canopy temperatures and climatic conditions at the study sites (King and Shellie, 2016). For sugarbeet, the database included measured canopy temperature from FIT plots at NWISRL from 2014 through 2019 and at PREC in 2018. For wine grape, the cultivar-specific databases included measured canopy temperature from FIT plots for Malbec and Syrah from 2014 through 2016 at UIPREC and for Pinot noir in 2015 and 2016 at UIPREC and in 2018 and 2019 at the Oregon site. Neural network model development was performed using the MATLAB Neural Network Toolbox (MathWorks, Natick, Mass.). The data were randomly subdivided into three datasets used to train, validate, and test the NN models. Half (50%) of the data were used for training, 25% for validation, and 25% for testing. Model parameters (R_s, T_a, RH, WS, and T_c) were linearly scaled to a range of -1 to +1 based on measured maximum and minimum values (table 1), which is a typical procedure to facilitate convergence to NN model solution, and the Levenberg-Marquardt backpropagation method was used to solve for model coefficients (MATLAB Neural Network Toolbox, MathWorks, Natick, Mass.). Hidden layer neurons in the NN model used a hyperbolic tangent activation function, and the single output neuron used a linear activation function. The NN model included only one hidden layer. The number of hidden neurons was selected by trial and error based on minimizing the sum of squared errors between measured and predicted T_{LL}, while using a minimum number of neurons to reduce the risk of over-training the NN model to the dataset. This resulted in NN models using four hidden neurons for sugarbeet and five hidden neurons for wine grape.

Non-transpiring canopy temperature (T_{UL}) was estimated using the approach of O'Toole and Real (1986) (eqs. 1 to 5) using measured well-watered canopy temperature of the FIT and associated climatic parameters. Regression analysis was applied to a multi-year dataset of well-watered canopy temperature and VPD to solve for coefficients *a* and *b* in equation 3. Average aerodynamic resistance ($\overline{r}_{ap}$) was calculated using equation 4 and regression values *a* and *b*. Equations given by ASCE (2005) were used to compute e_s, e_a, $\overline{\Delta}$, and $\overline{\rho}$ from measured T_a and RH. Average net radiation ($\overline{R}_n$)was estimated as a linear function of R_s based on net radiation measurements collected in other field studies of sugarbeet and wine grape by the authors. Non-transpiring canopy temperature (T_{UL}) was calculated for a 15 min period using equation 2 with $\overline{r}_{ap}$ and calculated 15 min average values for R_s and ρ from measured 15 min average values of R_s, T_a, and RH.

The integrity of the measured canopy temperature data was evaluated to ensure that only dry canopy conditions were included in the dataset used for T_{LL} NN model development and evaluation and determination of $\overline{r}_{ap}$. This was accomplished by omitting measured canopy temperature data for times of suspected wet canopy conditions based on rain gauge data and irrigation records.

Daily canopy temperature and climatic conditions within -1 to +2.5 h of solar noon were used in this study to characterize water stress. In sugarbeet, wilting is prevalent after solar noon when water stressed, with the duration and frequency of wilting indicative of tuber and sucrose yield impacts (Martin et al., 2007). This characteristic wilting suggests that -1 to +2.5 h of solar noon is when canopy temperature might be most indicative of plant water stress. The diurnal trend in LWP of wine grape is a minimum near solar noon and has been found to be well correlated with canopy temperature (van Zyl, 1987). The characteristic minimum LWP near solar noon is the basis for the use of midday LWP or SWP as a standard measure of grape vine water stress for irrigation management (Levin, 2019; Williams and Baeza, 2007). Based on this information, data within -1 to +2.5 h of solar noon were selected to quantify plant water stress using canopy temperature. Models to estimate T_{LL} and T_{UL} were developed using measured data (R_s, T_a, RH, and WS) within -1 to +2.5 h of solar noon in their development. Consequently, model predictions are only valid for this time frame.

Table 1. Maximum and minimum measured values for climatic parameters and canopy temperature used in development of neural network models for predicting well-watered canopy temperature of sugarbeet and Pinot noir wine grape.

	Solar Radiation ($W\ m^{-2}$)		Air Temperature (°C)		Relative Humidity (%)		Wind Speed ($m\ s^{-1}$)		Canopy Temperature (°C)	
Crop	Max	Min	Max	Min	Max	Min	Max	Min	Max	Min
Sugarbeet	1120	28	36.4	7.7	99	7	8.6	0.3	28.8	7.1
Pinot noir	1038	31	37.0	14.5	61	10	5.3	0.3	34.3	16.2

A daily CWSI value was calculated as the average of the twelve 15 min computed CWSI values between 13:00 and 16:00 MDT for sugarbeet and the average of the nine 15 min computed CWSI values between 13:00 and 15:00 local daylight time for wine grape. The shorter time interval for wine grape corresponded to -1 to + 1.5 h of solar noon and was selected to reduce the possibility of leaf shading based on visual observations.

Model Evaluation

The effectiveness of model predictions for T_{LL} was assessed using four goodness-of-fit measures: Nash-Sutcliffe model efficiency (NSE), mean absolute error (MAE), root mean squared error (RMSE), and percent bias (PBIAS). The NSE is a normalized statistic that expresses the relative magnitude of the residual variance to the measured data variance (Nash and Sutcliffe, 1970). It is defined as:

$$\mathrm{NSE} = 1 - \frac{\sum_{i=1}^{n}\left(O_i - P_i\right)^2}{\sum_{i=1}^{n}\left(O_i - \bar{O}\right)^2} \tag{6}$$

where

P_i = model prediction for a measured value (O_i)

$\bar{O}$ = mean of the measured values

n = number of values.

The NSE quantifies the predictive efficacy of a model and can range from –∞ to 1, where a value of 1 indicates $P_i = O_i$ for all measured data. A value nearer 1 indicates better model prediction efficacy. A negative value indicates that the mean of the observations is a better predictor of O_i than the model.

The MAE quantifies the average magnitude of model prediction error absolute values. It is defined as:

$$\mathrm{MAE} = \frac{\sum_{i=1}^{n}\left|P_i - O_i\right|}{n} \tag{7}$$

A smaller MAE indicates better model prediction performance.

The RMSE is the sample standard deviation of the differences between predicted and observed values. It is defined as:

$$\mathrm{RMSE} = \sqrt{\frac{\sum_{i=1}^{n}\left(P_i - O_i\right)^2}{n}} \tag{8}$$

A smaller RMSE indicates better model prediction performance.

The PBIAS is a measure of how much the fitted model over- or underpredicts the observed values. The PBIAS is calculated as (Yapo et al., 1996):

$$\mathrm{PBIAS} = \left[\frac{\sum_{i=1}^{n}\left(P_i - O_i\right)}{\sum_{i=1}^{n} O_i}\right] \times 100 \tag{9}$$

Values for PBIAS range from -∞ to ∞, with an optimal value of zero; however, values close to zero can occur if the fitted model overpredicts as much as it underpredicts (Moriasi et al., 2007).

Data Analysis

Linear and multiple linear regression was conducted using Microsoft Excel data analysis tools. Graphical, linear, and multiple linear regression and variance analysis were used to quantify and evaluate the performance of the prediction models. Regression line significance was evaluated using ANOVA ($p \le 0.05$). Equality of variances was evaluated using a Levine test when data were normally distributed and a non-parametric Levene test (Nordstokke and Zumbo, 2010; Nordstokke et al., 2011) when data were not normally distributed. Normal Q-Q plots, histograms, and Shapiro-Wilk tests ($p \le 0.05$) were used to assess if data were approximately normally distributed. Graphs were generated using Sigmaplot 14 (Systat Software, San Jose, Cal.).

Results and Discussion

Sugarbeet

The study sites had a wide range of climatic conditions (table 1), leading to a wide range in VPD (fig. 1) and measured well-watered canopy temperatures (table 1) in the FIT plots. The linear correlation between $T_c - T_a$ and VPD measured between 13:00 and 16:00 MDT was significant ($p \le 0.001$), with a coefficient of determination (R^2) of 0.70 (fig. 1). The high degree of variability shown in figure 1 for $T_c - T_a$ at any given value of VPD illustrates a strong influence of additional factors on leaf temperature other than soil water availability. The small grouping of data values above the bulk data at VPD of ~3.7 kPa occurred during a high wind event exceeding 6 m s-

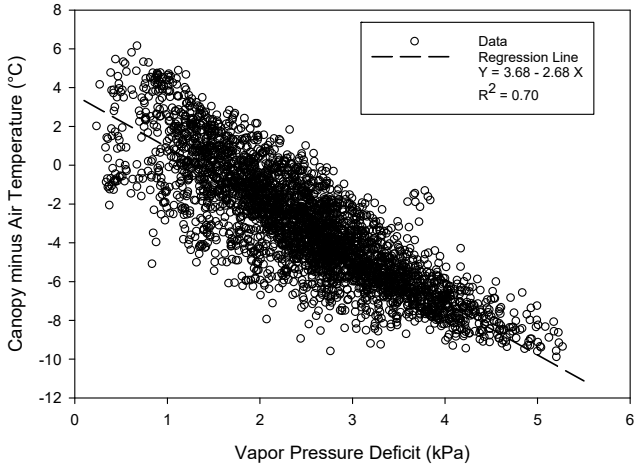

Figure. 1. Relationship between measured canopy temperature minus air temperature and vapor pressure deficit for sugarbeet in fully irrigated treatments (FIT) at both study sites (n = 3386).

[1] at site 1, which may have decreased stomatal conductance, reducing the transpiration rate and increasing canopy temperature despite adequate soil water availability.

The NN model developed to predict T_{LL} using input variables T_a, R_s, RH, and WS measured between 13:00 and 16:00 MDT was significant ($p \leq 0.001$), with a coefficient of determination (R^2) of 0.88 between measured and predicted T_{LL} (fig. 2) in the FIT plots. The NN model was a much better predictor of T_{LL} than a linear model. The NSE, RMSE, MAE, and PBIAS of the NN model were 0.88, 1.07°C, 0.82°C, and 0, respectively. For the NN model, all the prediction performance parameters were equal to or better than the results for a multiple linear regression (MLR) model (data not shown), indicating that NN modeling was better than MLR for predicting T_{LL}. The linear regression equation slope for predicted versus measured T_{LL} was significantly ($p < 0.001$) different from 1 (0.87, fig. 2), indicating a bias in predictions despite PBIAS = 0. The NN model overpredicted T_{LL} for well-watered canopy temperatures <20°C and underpredicted for well-watered canopy temperatures >25°C.

The dataset used to determine the linear relationship between $T_c - T_a$ and VPD (eq. 3) for estimating average aerodynamic resistance ($\overline{r}_{ap}$ in eq. 4) is shown in figure 3. The difference between the datasets in figures 1 and 3 is the removal of $T_c - T_a$ when R_s was <750 W m^{-2} to eliminate the possible inclusion of data when canopy resistance was increased due to reduced sunlight and actual ET was less than potential ET. Data values for high wind conditions (WS > 5.5 m s^{-1}) were also removed to eliminate the possible influence of high wind on canopy resistance. Linear regression of the resulting $T_c - T_a$ versus VPD dataset (fig. 3), with coefficient of determination (R^2) of 0.85 ($p < 0.001$), resulted in a slope of 3.02°C kPa^{-1} and intercept of 4.92°C. Dataset (fig. 3) values for $\overline{\Delta}$, $\overline{\gamma}$, and $\overline{\rho}$ were 212.8 Pa °C^{-1}, 60.6 Pa °C^{-1}, and 1.05 kg m^{-3}, respectively, and the value of c_p was taken as 1013 J kg^{-1} °C^{-1}. Net radiation was not directly measured in any study year but calculated from measured 15 min averaged data collected at PREC in 2017 as part of a Bowen ratio study in sugarbeet. The linear relationship between measured R_n and R_s at PREC was $R_n = 0.65R_s + 14.7$, with an R^2 of 0.95.

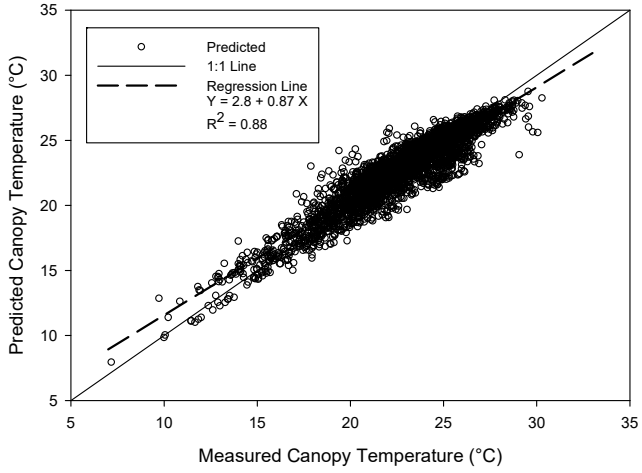

Figure 2. Neural network (NN) prediction of sugarbeet canopy temperature (T_{LL}) compared to measured canopy temperature in fully irrigated treatments (FIT) at both study sites (n = 3386).

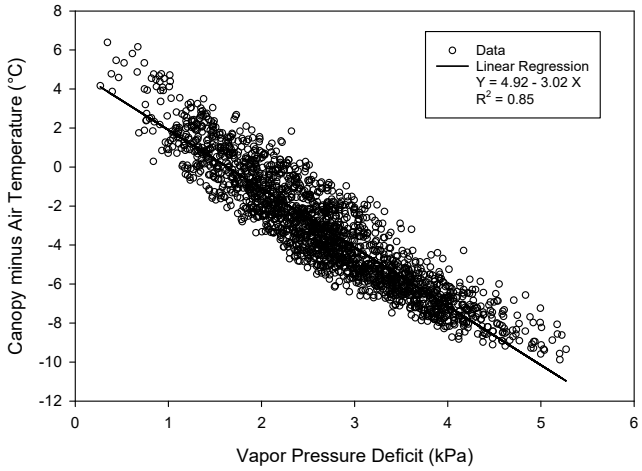

Figure 3. Relationship between measured canopy temperature minus air temperature and vapor pressure deficit for sugarbeet in fully irrigated treatments (FIT) and linear relationship used to estimate upper reference temperature (T_{UL}) for both study sites (n = 1989).

This relationship was used to calculate R_n from 15 min averaged values of R_s for both sites. Based on this relationship, the dataset (fig. 3) value for $\overline{R}_n$ was 573 W m^{-2}. Substituting dataset average values into equations 4 and 5 resulted in $\overline{r}_{ap}$ = 25.4 s m^{-1} and $\overline{r}_{cp}$ = 24.4 s m^{-1}. Substituting the appropriate values into equation 2 resulted in $T_{UL} - T_a$ = 13.7°C. These values are quite sensitive to the slope and intercept of the regression equation through the dataset. Using sugarbeet canopy temperature data from Idso (1982), O'Toole and Real (1986) calculated $\overline{r}_{ap}$ = 8.8 s m^{-1} and $\overline{r}_{cp}$ = 37.6 s m^{-1}, which leads to $T_{UL} - T_a$ of about 4.5°C, substantially less than the 13.7°C obtained in this study. The dataset of Idso (1982) was comprised of 47 data values over a VPD range of 1.5 to 4.1 kPa, resulting in a regression slope of -1.96°C kPa^{-1}, which is much less than the slope found in this study using 1989 data values spanning a larger range in VPD. The dataset of Sepaskhah et al. (1988) was comprised of 77 values over a VPD range of 1.4 to 4.8 kPa, resulting in a regression slope of -2.6, which for the average climatic conditions of this study resulted in $T_{UL} - T_a$ = 8.5°C. The datasets of Idso (1982) and Sepaskhah et al. (1988) are enveloped within the dataset collected in this study (fig. 3). The sensitivity of $T_{UL} - T_a$ to regression line slope underscores the need for a large dataset over a wide range in VPD to obtain a reliable estimate of $T_{UL} - T_a$ using the approach of O'Toole and Real (1986). Data over a limited range in VPD are not adequate for reliable estimation of $T_{UL} - T_a$. The regression line slope is sensitive to data for VPD < 1.5 kPa.

Measured $T_c - T_a$ versus VPD for $R_s \geq 750$ W m^{-2} (fig. 3) diverged from a linear relationship for VPD < 1.0 kPa and for VPD > 4.5 kPa. A quadratic equation provided a slightly better fit (R^2 = 0.86, not shown) to the data than a linear equation. When VPD is <1.0 kPa, the vapor pressure gradient across the leaf surface boundary begins to limit the latent heat transfer rate, causing the leaf surface temperature to increase to maintain the energy balance between radiant, latent, and convective heat exchange with the environment. When VPD is >4.5 kPa, latent heat transfer (transpiration) becomes limited

by energy availability, limiting cooling and resulting in a lower limit for $T_{LL} - T_a$. The dataset of Sepaskhah et al. (1988) had a similar trend for VPD > 4.5 kPa.

Values of CWSI at 15 min periods between 13:00 and 16:00 MDT were calculated for all irrigation treatments using the NN model to predict T_{LL} for measured 15 min average values of R_s, T_a, RH, and WS, and T_{UL} was calculated (eq. 2) using 15 min average values for R_n and ρ and $\overline{r}_{ap}$ = 25.4 s m^{-1}.

Daily CWSI values for sugarbeet calculated with the methods developed in this study are shown in figures 4 and 5 for the NWISRL and PREC sites, respectively. Example daily CWSI values, computed as the average 15 min CWSI between 13:00 and 16:00 MDT, are shown in figure 4 along with daily irrigation plus precipitation amounts and available soil water (ASW) for the 25% FIT in 2015 at NWISRL. Daily CWSI was <0.1 before mid-July and rapidly increased and oscillated between 0.2 and 0.4 in response to small frequent irrigation amounts until mid-August. Daily CWSI then increased to 0.5 by the end of August in response to about a week without irrigation when ASW decreased to <45%. Daily CWSI remained below 0.4 through mid-September despite continued decrease in ASW below 45%. This is likely due to a gradual reduction in daily ET rate near the end of the growing season and rehydration of the crop overnight, supported by a 2.2 m root zone depth. Daily CWSI briefly decreased to 0.1 in mid-September in response to precipitation, reduced ET, and irrigation. Daily CWSI then rapidly increased to 0.5 by the end of September due to withheld irrigation for a week and ASW well below 45%. Over the season, daily CWSI decreased minimally following an irrigation event due to the small irrigation applications (<8 mm) by the lateral-move irrigation system. The minimal reduction in daily CWSI from irrigation likely resulted from a substantial fraction of applied water evaporating from the crop and soil surface rather than entering the soil profile.

Daily CWSI at PREC in 2018 for the 60% FIT treatment (fig. 5) varied between 0 and 0.9 in response to water application. Daily CWSI was >0.8 in mid-July due to lack of irrigation resulting from an irrigation equipment failure at the end of June. Available soil water was below 45% in mid-July (fig. 5), resulting in daily CWSI exceeding 0.8. Daily CWSI rapidly decreased to <0.1 by the end of July due to several irrigation events. Available soil water stabilized but did not substantially increase. In the first week of August, daily CWSI rapidly increased to nearly 0.8 when irrigation frequency decreased. Three irrigations between 18 and 27 July, which rapidly decreased daily CWSI, likely restored soil water in the top 0.15 m of the soil profile that was not fully detected by the neutron probe soil water measurements. Limited soil water stored in the 0.15 m soil profile was readily removed by the sugarbeet crop, and daily CWSI rapidly increased during early August. Two irrigation events between 10 and 15 August stabilized daily CWSI, and the two irrigations between 16 and 20 August decreased daily CWSI to zero and increased ASW slightly. During the first ten days of September, daily CWSI rapidly increased to 0.8 due to the lack of irrigation, which likely depleted soil water in the top 0.15 m of the soil profile and decreased measured soil water content. Available soil water reached a minimum on 11 September, and daily CWSI reached a maximum of 0.9. Daily CWSI was much more dynamic at PREC than at NWISRL due to limited soil water storage resulting from less water holding capacity of the gravelly loam soil profile and the <1 m root zone depth.

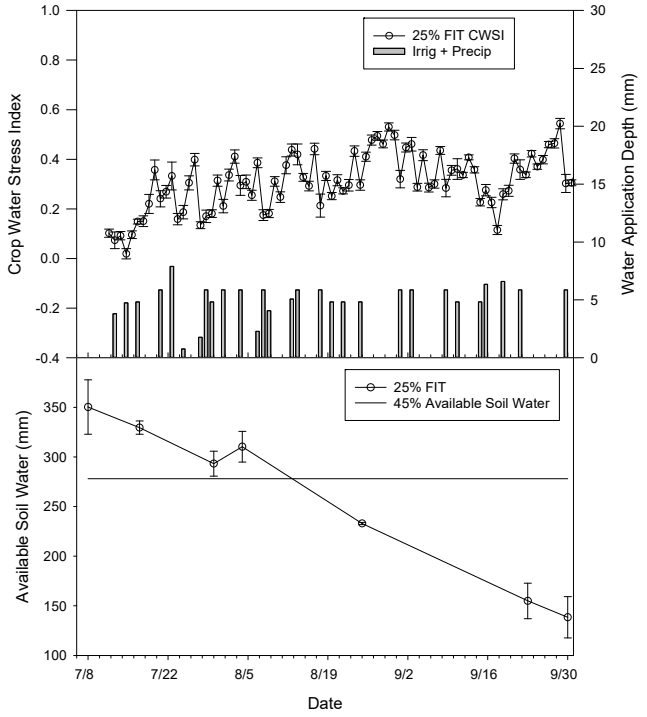

Figure 4. Crop water stress index and available soil water of sugarbeet in response to irrigation timing and amounts to the 25% FIT at NWISRL (Kimberly, Ida.) in 2015. Vertical bars represent standard errors of the measurements.

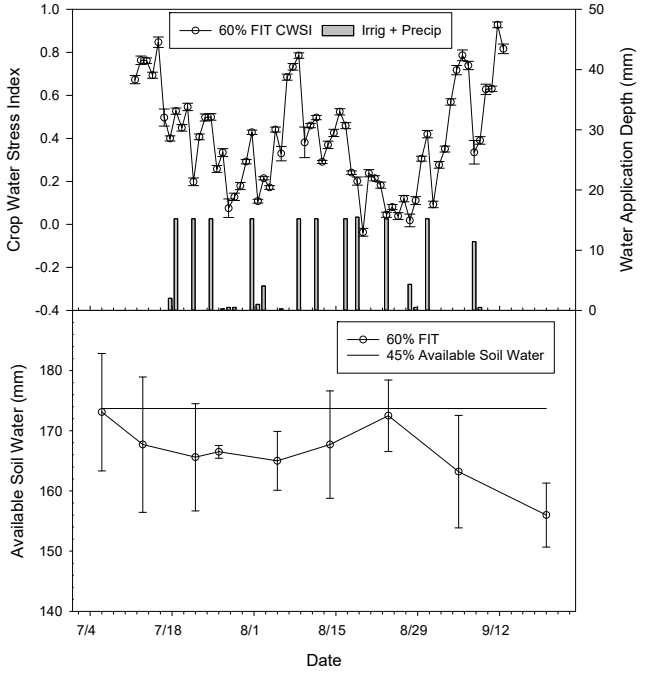

Figure 5. Crop water stress index and available soil water of sugarbeet in response to irrigation timing and amounts of the 60% FIT at PREC (Powell, Wyo.) in 2018. Vertical bars represent standard errors of the measurements.

WINE GRAPE

The study sites for Pinot noir had very similar growing season climatic conditions, potentially limiting transferability of derived data-driven models to a reduced range of climatic conditions compared to that for sugarbeet. The primary deficiency was an absence of measured data for VPD < 1.0 kPa (fig. 6). The linear correlation between $T_c - T_a$ and VPD measured between 13:00 and 15:00 local daylight time for Pinot noir was significant ($p \leq 0.001$), with a coefficient of determination (R^2) of 0.54 (fig. 6). The linear relationship was very similar to that reported by Bellvert et al. (2014) for Pinot noir in the first year of their study. The high degree of variability for $T_c - T_a$ at any given value of VPD illustrates a strong influence of additional factors on leaf temperature other than soil water availability. Similar relationships were found between $T_c - T_a$ and VPD for wine grape cultivars Malbec, Syrah, Merlot, Chardonnay, Cabernet Franc, and Cabernet Sauvignon (data not shown) grown at UIPREC.

The NN model developed to predict T_{LL} using input variables T_a, R_s, RH, and WS measured between 13:00 and 15:00 local daylight time was significant ($p \leq 0.001$), with a coefficient of determination (R^2) of 0.90 between measured and predicted T_{LL} (fig. 7). The NSE, RMSE, MAE, and PBIAS of the NN model were 0.90, 0.98°C, 0.74°C, and 0.2, respectively. The linear regression equation slope for predicted versus measured T_{LL} was significantly ($p \leq 0.001$) different from 1 (0.89, fig. 7), indicating a bias in predictions despite PBIAS = 0.2. The NN model overpredicted well-watered canopy temperatures <25°C and underpredicted well-watered canopy temperatures >30°C.

The dataset (fig. 8) used to estimate T_{UL} based on the approach of O'Toole and Real (1986) (eqs. 1 to 5) differs from figure 7 due to the removal of $T_c - T_a$ when R_s was <750 W m^{-2} to eliminate the possible inclusion of T_c values where actual ET was less than potential ET. Linear regression of the dataset in figure 8 ($R^2 = 0.71$, $p \leq 0.001$) resulted in a slope of -1.85°C kPa^{-1} and intercept of 4.85°C. The linear relationship is nearly identical to the two-year average reported by Bellvert (2014) for Pinot noir. The resulting linear regression line does not visually represent the trend in the data but minimizes the sum of squared prediction errors associated with the specific dataset. Thus, estimation of T_{UL} using the linear regression model will likely result in the estimated value being specific for the data collected in this study, limiting transferability to other regions. The lack of canopy temperature measurements for VPD < 1 kPa greatly increases the likelihood of the linear regression line erroneously representing the underlying trend in the data. A possible solution to this issue is to use a linear model of the data that maximizes the correlation coefficient (Livadiotis and McComas, 2013). Maximizing the correlation coefficient of a linear line through the dataset resulted in a slope of 2.50°C kPa^{-1} and intercept of 6.2°C, with an R^2 of 0.79. Had canopy temperature measurements been collected for VPD < 1 kPa, based on the dataset for sugarbeet (fig. 3), the linear model corresponding to maximizing the correlation coefficient would likely be a better representation of the data than the linear regression line. Incidentally, the linear regression line for sugarbeet (fig. 3) also maximized the correlation coefficient. Dataset (fig. 8) values for $\overline{\Delta}$, $\overline{\gamma}$, and $\overline{\rho}$ were 230.0 Pa

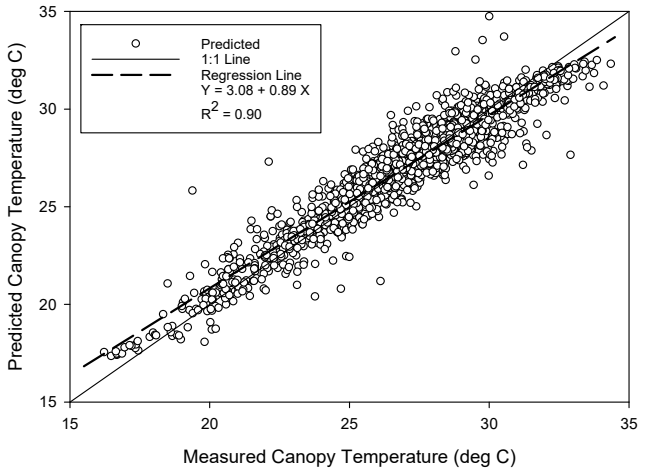

Figure 7. Neural network (NN) prediction of Pinot noir canopy temperature (TLL) compared to measured canopy temperature in fully irrigated treatments (FIT) at both study sites (n = 1779).

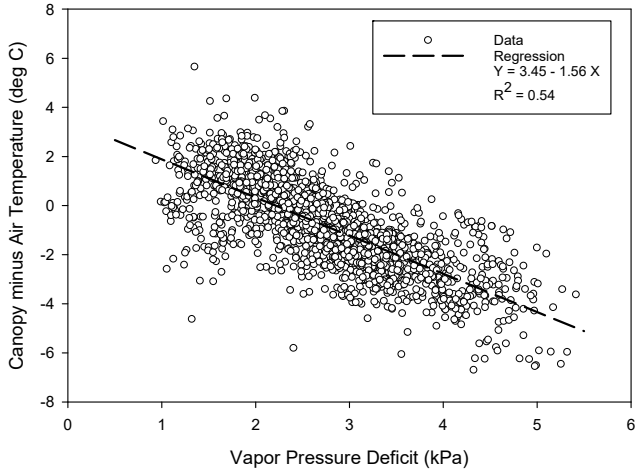

Figure 6. Relationship between measured canopy temperature minus air temperature and vapor pressure deficit for Pinot noir wine grape in fully irrigated treatments (FIT) at both study sites (n = 1779).

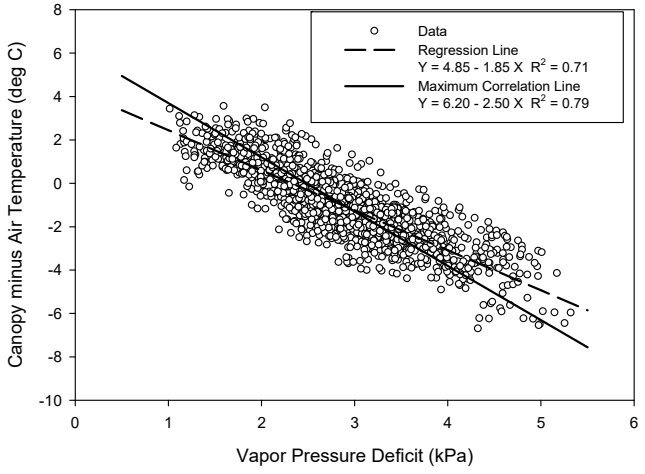

Figure 8. Relationship between measured canopy temperature minus air temperature and vapor pressure deficit for Pinot noir wine grape in fully irrigated treatments (FIT) and linear relationship used to estimate upper reference temperature (T_{UL}) for both study sites (n = 1417).

°C^{-1}, 59.0 Pa °C^{-1}, and 1.01 kg m^{-3}, respectively, and the value of c_p was taken as 1013 J kg^{-1} °C^{-1}. Net radiation of Malbec vines was measured in 2018 and 2019 at UIPREC. The linear relationship between measured R_n and R_s at UIPREC was $R_n = 0.9R_s - 60$, with an R^2 of 0.95. This relationship was used to calculate R_n from 15 min averaged values of R_s for both study sites. Based on this relationship, the value for $\overline{R}_n$ was 711 W m^{-2} for the dataset in figure 8. Substituting dataset average values into equations 4 and 5 resulted in $\overline{r}_{ap}$ = 21 s m^{-1} and $\overline{r}_{cp}$ = 39.6 s m^{-1}. Substituting the appropriate values into equation 2 resulted in $T_{UL} - T_a$ = 14.6°C. This is double the value for $T_{UL} - T_a$ used by Bellvert (2014) to calculate the CWSI of Pinot noir.

The approach of O'Toole and Real (1986) (eqs. 1 to 5) was also used to estimate T_{UL} for wine grape varieties Malbec and Syrah grown at UIPREC. Measured canopy temperature datasets for R_s > 750 W m^{-2} are shown in figures 9 and 10 for Malbec and Syrah, respectively. A linear model that maximizes the correlation coefficient for the dataset was used to estimate T_{UL}. The linear model for Malbec had a slope of -2.33°C kPa^{-1} and intercept of 5.1°C, with an R^2 of 0.78 (fig. 9), and the linear model for Syrah had a slope of -2.2°C kPa^{-1} and intercept of 4.6°C, with an R^2 of 0.79 (fig. 10). Dataset values for $\overline{\Delta}$, $\overline{\gamma}$, and $\overline{\rho}$ for both Malbec and Syrah were 229.3 Pa °C^{-1}, 63.0 Pa °C^{-1}, and 1.08 kg m^{-3}, respectively, and the value of c_p was taken as 1013 J kg^{-1} °C^{-1}. The value for $\overline{R}_n$ was 702 W m^{-2} for both Malbec and Syrah. Substituting dataset average values into equations 4 and 5 resulted in $\overline{r}_{ap}$ = 16.8 s m^{-1} and $\overline{r}_{cp}$ = 34.5 s m^{-1} for Malbec and $\overline{r}_{ap}$ = 14.5 s m^{-1} and $\overline{r}_{cp}$ = 37.4 s m^{-1} for Syrah. Substituting the appropriate values into equation 2 resulted in $T_{UL} - T_a$ = 11.4°C for Malbec and 9.3°C for Syrah. Computed values of $T_{UL} - T_a$ are very sensitive to the slope and intercept of the linear models selected for $T_c - T_a$ versus VPD.

Daily CWSI values for Malbec 70% FIT and 35% FIT at UIPREC in 2015 computed as the average 15 min CWSI between 13:00 and 15:00 MDT are shown in figure 11 along with daily irrigation and precipitation amounts. Wine grape irrigation in the region normally begins near the first week in July after fruit set. Daily CWSI for 35% FIT was near 0.6 when canopy temperature measurement started and then decreased slightly following irrigation events exceeding 35 mm in the first half of August. Daily CWSI for 35% FIT remained <0.5 through September but increased after irrigation was terminated at the end of September. The daily CWSI pattern for 70% FIT was similar to that of 35% FIT, as it decreased in the last half of July to <0.3 in response to irrigation events exceeding 50 mm. The daily CWSI for 70% FIT then increased to nearly equal the daily CWSI for 35% FIT through mid-September. The 50% difference in irrigation amounts between 35% and 70% FIT only resulted in minimal differences in daily CWSI between treatments through mid-September. Daily CWSI of both irrigation treatments decreased following an irrigation event. However, the CWSI of 35% FIT increased sooner and more rapidly after an irrigation event due to half as much irrigation applied. Daily CWSI showed the dynamic interaction between irrigation, soil water availability, and plant water stress throughout the irrigation season.

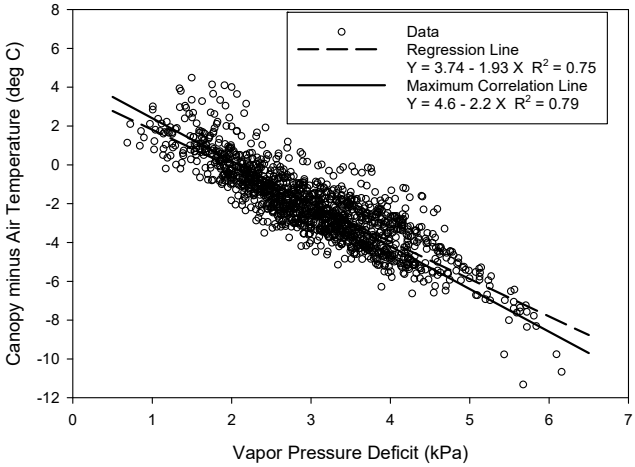

Figure 10. Relationship between measured canopy temperature minus air temperature and vapor pressure deficit for Syrah wine grape in fully irrigated treatments (FIT) and linear relationship used to estimate upper reference temperature (T_{UL}) (n = 1345).

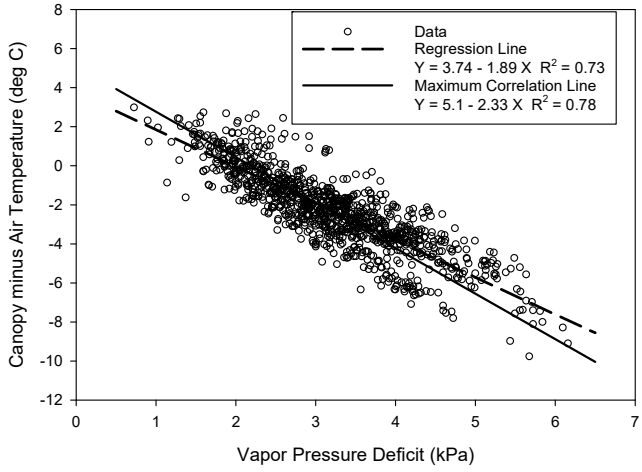

Figure 9. Relationship between measured canopy temperature minus air temperature and vapor pressure deficit for Malbec wine grape in fully irrigated treatments (FIT) and linear relationship used to estimate upper reference temperature (T_{UL}) (n = 1023).

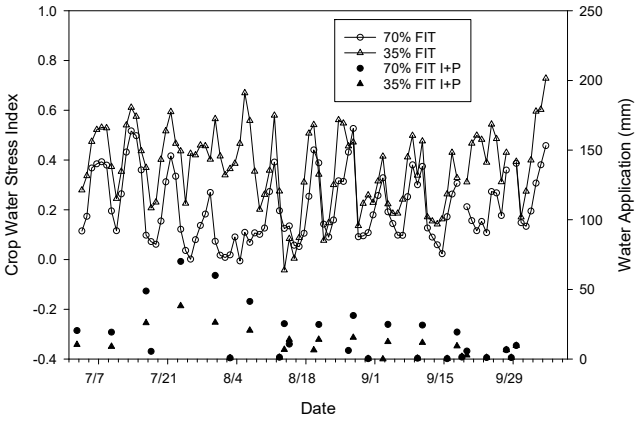

Figure 11. Crop water stress index of Malbec wine graph at Parma, Idaho, in 2014 in response to irrigation timing and amounts for 70% FIT and 35% FIT (I+P = irrigation plus precipitation).

The relationship between daily CWSI and midday leaf water potential (LWP) of Malbec and Syrah at UIPREC over a three-year period (2014, 2015, and 2016) is shown in figure 12. A linear relationship between daily CWSI and LWP was significant ($p < 0.001$), with an R^2 of 0.53. A quadratic relationship between CWSI and LWP averaged over four wine grape cultivars was reported by Bellvert et al. (2015). Despite a significant linear relationship between CWSI and LWP (fig. 12), there is considerable variability in the relationship, which precludes use of CWSI as a direct surrogate for LWP. The same degree of variability was present in the relationship reported by Bellvert et al. (2015). One source of variability in the relationship is the operator judgement aspect of LWP and SWP measurements (Levin, 2019). Multiple operators collected LWP measurements at UIPREC in 2016, which likely introduced some variability in the LWP measurements. Williams and Baeza (2007) reported LWP ranging from -0.51 to -1.15 MPa for well-watered grapevines in California, with LWP linearly related to VPD and T_a. They also reported a linear relationship between LWP and VPD for water-stressed vines, but with reduced dependence on VPD compared to well-watered vines. The results of this study are consistent with the findings of Williams and Baeza (2007), as the relationship between CWSI and LWP (fig. 12) could be represented by a piece-wise linear relationship with CWSI ≈ 0 for LWP > -1.15 MPa. Solar radiation also influences LWP (Williams and Baeza, 2007), and LWP measurements should be collected on cloudless days. The LWP values reported in this study were made over a wide range in VPD and on days with variable clouds. The combination of multiple operators and a wide range in VPD, solar radiation, temperature, and evaporative demand during LWP measurements accounts for some of the variability in the relationship between CWSI and LWP. Additionally, some LWP values reported in this study were not collected on the same vine used for canopy temperature measurement, another source of variability in the relationship between CWSI and LWP (fig. 12). Overall, the presence of water stress detected by LWP measurement was also indicted by daily CWSI as calculated in this study, demonstrating that CWSI can be effectively used as an irrigation management tool for wine grape. The primary advantage of using CWSI as an irrigation management tool is the ability to automate data collection for daily monitoring of water stress with minimal labor.

The interaction between midday stem water potential (SWP) and average daily CWSI of Pinot noir at the southwest Oregon study site is shown in figure 13 for two irrigation treatments. For 25% FIT, daily CWSI was <0.1 at the end of June and steadily increased to 0.4 by the end of July. Concurrently, SWP was greater than -0.6 MPa at the end of June and steadily decreased to -1.4 MPa by the end of July. Near the first of August, an irrigation event quickly decreased the daily CWSI to <0.1, and SWP increased to exceed -0.7 MPa. During the first half of August, daily CWSI rapidly increased to 0.6, and SWP decreased to less than -1.4 MPa. From mid-August through mid-September, daily CWSI decreased to <0.1, and SWP increased to -0.6 MPa. For the 25% late deficit irrigation treatment (LD25), daily CWSI was near 0.2 through mid-July, and SWP was greater than -0.6 MPa. Throughout July, the CWSI ranged between 0.2 and 0.4, and SWP ranged between -1.3 and -0.6 MPa. In mid-August, daily CWSI increased to 0.7, and SWP decreased to -1.4 MPa. Daily CWSI then decreased to <0.3, and SWP increased to -0.6. In general, an increase in daily CWSI was accompanied by a decrease in SWP in the irrigation treatments, indicating that daily CWSI was an effective indicator of vine water stress at the Oregon study site.

The data-driven models developed in this study to estimate reference temperatures (T_{LL} and T_{UL}) permit calculation of CWSI for effective assessment of crop water stress with minimal labor requirement. The methodology used in this study to calculate daily CWSI can be automated for use as a

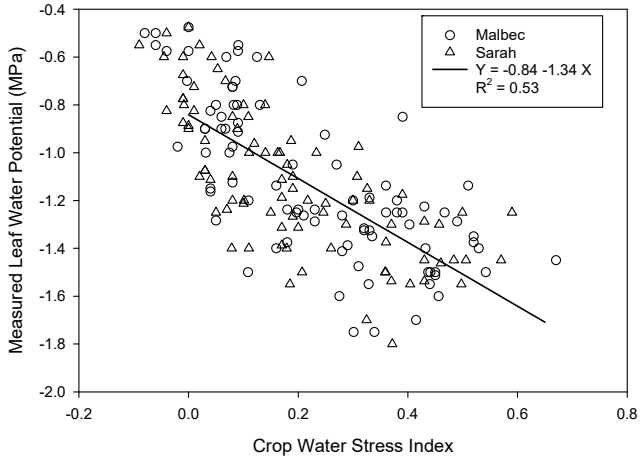

Figure 12. Relationship between crop water stress index and midday leaf water potential for Syrah and Malbec wine grape at Parma, Idaho, over three years (2014, 2015, and 2016).

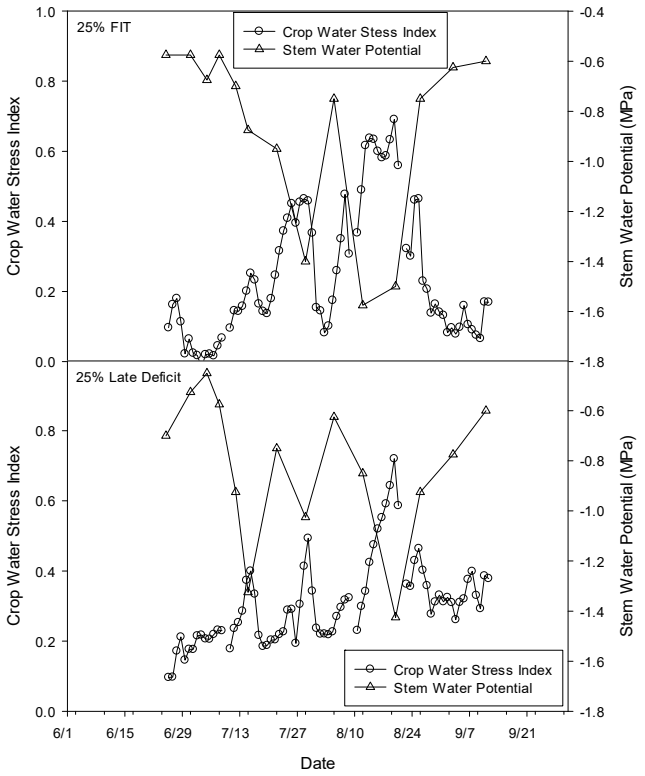

Figure 13. Relationship between crop water stress index and midday stem water potential for Pinot noir wine grape under two irrigation treatments (25% FIT and LD25) in southwestern Oregon in 2019.

daily irrigation management tool; however, the methodology is not fool-proof. The CWSI value can be less than zero or greater than one (<0 or >1) under certain conditions. Wet canopy conditions result in measured canopy temperature less than T_{LL} predicted by the NN model. This results in a negative CWSI value, preventing assessment of crop water stress, regardless of soil water availability. The original development of the CWSI concept by Idso et al. (1981) was limited to clear sunny conditions. However, the data-driven NN models developed in this study are based on well-watered canopy temperatures measured under variable cloudy conditions and predict T_{LL} for variably cloudy conditions, enhancing the efficacy of the CWSI concept. While the NN models developed for predicting T_{LL} are valid for solar radiation <100 W m^{-2} (table 1), T_{UL} predicted using equation 2 for low levels of solar radiation can be approximately equal to T_{LL}, resulting in CWSI values <0 or >1. In this study, solar radiation <200 W m^{-2} often resulted in CWSI values <0 or >1. Bockhold (2011) also found that solar radiation >200 W m^{-2} was necessary to reliably use canopy temperature measurement for irrigation scheduling. Automated calculation of CWSI using the methodology of this study would need to check for wet canopy or low solar radiation conditions and omit calculation of CWSI for the day if determined to be problematic.

Use of the methodology proposed by O'Toole and Real (1986) to estimate T_{UL} for sugarbeet and multiple wine grape cultivars in this study resulted in average values of T_{UL} that were approximately double the values used in other studies. Rather than using traditional regression to fit a linear model to measured data, a linear model that maximized the correlation coefficient was used for wine grape due to the absence of measured data for VPD < 1 kPa. The method of O'Toole and Real (1986) uses the slope and intercept of a linear model of measured data to estimate an average value for r_a in equation 4. A linear model that estimates the underlying trend in measured data is needed to provide an estimate of $\overline{r}_{ap}$ that is transferrable to other regions. Linear regression is strictly dependent on measured data and can be a biased estimate of the underlying trend in the dataset, particularly if only a small number of values are collected or if the measured data do not include the complete range of the possible values. In this study, measured data for sugarbeet included nearly the complete range of VPD values possible; hence, the linear regression model also maximized the correlation coefficient and captured the underlying trend in the data. This was not the case with wine grape, so a linear model that maximized the correlation coefficient was used to estimate r_a to increase the likelihood of transferability to other regions. Estimates of r_a using a linear model that maximizes the correlation coefficient between $T_{LL} - T_a$ and VPD resulted in values of T_{UL} consistent with the maximum measured values of T_c in severely water-stressed plots and constrained the computed values of CWSI within the range of 0 to 1 in these cases, validating the values of T_{UL} obtained in this study.

The models developed in this study and their demonstrated performance are based on historical data collected at multiple locations. These models can be directly applied to estimate T_{LL} and T_{UL} of sugarbeet and wine grape cultivars Pinot noir, Malbec, and Syrah in irrigated regions of the northwestern U.S. The models can be readily incorporated into CWSI-based irrigation scheduling models applied to these crops in the region. The models can also be easily incorporated into standalone spreadsheet models to estimate T_{LL} and T_{UL} of these crops. The models can be extended to other locations by addition of a few hundred data values (R_s, T_a, RH, WS, and T_{LL}) collected at the new location for each crop. The modeling concepts can be readily extended to other crops by collection of addition crop-specific data (R_s, T_a, RH, WS, and T_{LL}).

CONCLUSIONS

Canopy temperatures of sugarbeet, grown in Idaho and Wyoming, and wine grape, grown in Idaho and Oregon, over five years under full and severe deficit irrigation were measured concurrent with climatic conditions. Neural network models were developed to estimate well-watered canopy temperature based on measured solar radiation, ambient air temperature, relative humidity, and wind speed. Neural network models with one hidden layer with four neurons for sugarbeet and five neurons for wine grape provided excellent predictions of well-watered canopy temperature. The NSE of the models were equal to or greater than 0.88, with RMSE was less than 1.1°C. The relationship between $T_{LL} - T_a$ and VPD was modeled using a linear function that maximized the correlation coefficient rather than minimizing the sum of squared prediction error to better estimate the overall trend in the relationship rather than maximize the fit to the measured data. The intercept and slope of the linear model were used to estimate the average aerodynamic resistance of the crop canopy, which was used to estimate T_{UL} as a function of net radiation, density of the air, and heat capacity of the air. Resulting values for T_{UL} were nearly double the values reported in previous studies of CWSI for irrigation management of sugarbeet and wine grape. Use of greater T_{UL} in this study resulted in CWSI values that are less sensitive to mild levels of water stress compared to other studies. Despite this reduction in sensitivity, severely water-stressed plots of sugarbeet and wine grape resulted in CWSI values exceeding 0.9. Thus, estimates of T_{UL} were appropriate for the conditions of this study.

Daily CWSI was calculated as the average of 15 min values determined between 13:00 and 16:00 MDT for sugarbeet and between 13:00 and 15:00 local time for wine grape. Daily CWSI values were well correlated with irrigation events and amounts. Daily CWSI decreased rapidly following an irrigation event and increased after an irrigation event at higher rates for smaller irrigation amounts. Daily CWSI for sugarbeet increased as ASW decreased. A linear relationship between daily CWSI and LWP for Malbec and Syrah wine grapes was significant ($p < 0.001$), with an R^2 of 0.53. There was considerable variability in the relationship, preventing the use of daily CWSI as a surrogate for LWP, but the significant correlation indicates that daily CWSI can be a useful tool for irrigation management of wine grape. Daily CWSI was also found to be well linked with SWP of Pinot noir grown in southwestern Oregon.

REFERENCES

Alchanatis, V., Cohen, Y., Cohen, S., Möller, M., Sprinstin, M., Meron, M., ... Sela, E. (2010). Evaluation of different approaches for estimating and mapping crop water status in cotton with thermal imaging. *Prec. Agric., 11*(1), 27-41. https://doi.org/10.1007/s11119-009-9111-7

ASCE. (2000). Artificial neural networks in hydrology: II. Hydrologic applications. *J. Hydrol. Eng., 5*(2), 124-137. https://doi.org/10.1061/(ASCE)1084-0699(2000)5:2(124)

ASCE. (2005). The ASCE standardized reference evapotranspiration equation. Reston, VA: ASCE Environmental and Water Resources Institute. Retrieved from https://epic.awi.de/id/eprint/42362/1/ascestzdetmain2005.pdf

Ashley, R. O., Neibling, W. H., & King, B. A. (1996). Irrigation scheduling using water use tables. CIS 1039. Moscow, ID: University of Idaho Cooperative Extension. Retrieved from https://www.extension.uidaho.edu/publishing/pdf/CIS/CIS1039.pdf

Bellvert, J., Marsal, J., Girona, J., & Zarco-Tejada, P. J. (2015). Seasonal evolution of crop water stress index in grapevine varieties determined with high-resolution remote sensing thermal imagery. *Irrig. Sci., 33*(2), 81-93. https://doi.org/10.1007/s00271-014-0456-y

Bellvert, J., Zarco-Tejada, P. J., Girona, J., & Fereres, E. (2014). Mapping crop water stress index in a 'Pinot-noir' vineyard: Comparing ground measurements with thermal remote sensing imagery from an unmanned aerial vehicle. *Prec. Agric., 15*(4), 361-376. https://doi.org/10.1007/s11119-013-9334-5

Bhakar, S. R., Ojha, S., Singh, R. V., & Ansari, A. (2006). Estimation of evapotranspiration for wheat crop using artificial neural network. *Proc. 4th World Conf. Computers in Agriculture* (305-314). St. Joseph, MI: ASABE.

Bockhold, D. L., Thompson, A. L., Sudduth, K. A., & Henggeler, J. C. (2011). Irrigation scheduling based on crop canopy temperature for humid environments. *Trans. ASABE, 54*(6), 2021-2028. https://doi.org/10.13031/2013.40654

Cohen, Y., Alchanatis, V., Meron, M., Saranga, Y., & Tsipris, J. (2005). Estimation of leaf water potential by thermal imagery and spatial analysis. *J. Exp. Bot., 56*(417), 1843-1852. https://doi.org/10.1093/jxb/eri174

Davenport, J. R., Stevens, R. G., & Whitley, K. M. (2008). Spatial and temporal distribution of soil moisture in drip-irrigated vineyards. *HortScience, 43*(1), 229-235. https://doi.org/10.21273/hortsci.43.1.229

DeJonge, K. C., Taghvaeian, S., Trout, T. J., & Comas, L. H. (2015). Comparison of canopy temperature-based water stress indices for maize. *Agric. Water Mgmt., 156*, 51-62. https://doi.org/10.1016/j.agwat.2015.03.023

Han, M., Zhang, H., Chavez, J. L., Ma, L., Trout, T. J., & DeJonge, K. C. (2018). Improved soil water deficit estimation through the integration of canopy temperature measurements into a soil water balance model. *Irrig. Sci., 36*(3), 187-201. https://doi.org/10.1007/s00271-018-0574-z

Hansen, B., Orloff, S., & Sanden, B. (2007). *Monitoring soil moisture for irrigation water management*. Davis, CA: University of California.

Hatfield, J. L. (1983). The utilization of thermal infrared radiation measurements from grain sorghum crops as a method of assessing their irrigation requirements. *Irrig. Sci., 3*(4), 259-268. https://doi.org/10.1007/BF00272841

Idso, S. B. (1982). Non-water-stressed baselines: A key to measuring and interpreting plant water stress. *Agric. Meteorol., 27*(1), 59-70. https://doi.org/10.1016/0002-1571(82)90020-6

Idso, S. B., Jackson, R. D., Pinter, P. J., Reginato, R. J., & Hatfield, J. L. (1981). Normalizing the stress-degree-day parameter for environmental variability. *Agric. Meteorol., 24*, 45-55. https://doi.org/10.1016/0002-1571(81)90032-7

Irmak, S., Haman, D. Z., & Bastug, R. (2000). Determination of crop water stress index for irrigation timing and yield estimation of corn. *Agron. J., 92*(6), 1221-1227. https://doi.org/10.2134/agronj2000.9261221x

Irmak, S., Payero, J. O., VanDeWalle, B., Rees, J., Zoubek, G., Martin, D. L., ... Leininger, D. (2016). Principles and operational characteristics of Watermark granular matrix sensor to measure soil water status and its practical applications for irrigation management in various soil textures. EC783. Lincoln, NE: University of Nebraska Extension. Retrieved from http://extensionpublications.unl.edu/assets/pdf/ec783.pdf

Jackson, R. D., Idso, S. B., Reginato, R. J., & Pinter Jr., P. J. (1981). Canopy temperature as a crop water stress indicator. *Water Resour. Res., 17*(4), 1133-1138. https://doi.org/10.1029/WR017i004p01133

Jones, H. G. (1992). *Plants and microclimate* (2nd ed.). Cambridge, UK: Cambridge University Press.

Jones, H. G. (1999). Use of infrared thermometry for estimation of stomatal conductance as a possible aid to irrigation scheduling. *Agric. Forest Meteorol., 95*(3), 139-149. https://doi.org/10.1016/S0168-1923(99)00030-1

Jones, H. G. (2004). Irrigation scheduling: Advantages and pitfalls of plant-based methods. *J. Exp. Bot., 55*(407), 2427-2436. https://doi.org/10.1093/jxb/erh213

Jones, H. G., Stoll, M., Santos, T., Sousa, C. d., Chaves, M. M., & Grant, O. M. (2002). Use of infrared thermography for monitoring stomatal closure in the field: Application to grapevine. *J. Exp. Bot., 53*(378), 2249-2260. https://doi.org/10.1093/jxb/erf083

Karasekreter, N., Basciftci, F., & Fidan, U. (2012). A new suggestion for an irrigation schedule with an artificial neural network. *J. Exp. Theor. Artif. Intel., 25*(1), 93-104. https://doi.org/10.1080/0952813X.2012.680071

King, B. A., & Shellie, K. C. (2016). Evaluation of neural network modeling to predict non-water-stressed leaf temperature in wine grape for calculation of crop water stress index. *Agric. Water Mgmt., 167*, 38-52. https://doi.org/10.1016/j.agwat.2015.12.009

Kumar, M., Raghuwanshi, N. S., Singh, R. V., Wallender, W. W., & Pruitt, W. O. (2002). Estimating evapotranspiration using artificial neural network. *J. Irrig. Drain. Eng., 128*(4), 224-233. https://doi.org/10.1061/(ASCE)0733-9437(2002)128:4(224)

Leinonen, I., & Jones, H. G. (2004). Combining thermal and visible imagery for estimating canopy temperature and identifying plant stress. *J. Exp. Bot., 55*(401), 1423-1431. https://doi.org/10.1093/jxb/erh146

Levin, A. D. (2019). Re-evaluating pressure chamber methods of water status determination in field-grown grapevine. *Agric. Water Mgmt., 221*, 422-429. https://doi.org/10.1016/j.agwat.2019.03.026

Li, T., Zhang, J.-f., Xiong, S.-y., & Zhang, R.-x. (2020). The spatial variability of soil water content in a potato field before and after spray irrigation in arid northwestern China. *Water Supply, 20*(3), 860-870. https://doi.org/10.2166/ws.2020.006

Livadiotis, G., & McComas, D. J. (2013). Fitting method based on correlation maximization: Applications in space physics. *J. Geophys. Res. Space Phys., 118*(6), 2863-2875. https://doi.org/10.1002/jgra.50304

Lo, T. H., Rudnick, D. R., Ge, Y., Heeren, D. M., Irmak, S., Barker, J. D., ... Shaver, T. M. (2018). Ground-based thermal sensing of field crops and its relevance to irrigation management. G2301. Lincoln, NE: University of Nebraska Extension. Retrieved from http://extensionpubs.unl.edu/publication/9000020029545/ground-based-thermal-sensing-of-field-crops-and-its-relevance-to-irrigation-management-g2301/

Maes, W. H., & Steppe, K. (2012). Estimating evapotranspiration and drought stress with ground-based thermal remote sensing in agriculture: A review. *J. Exp. Bot., 63*(13), 4671-4712. https://doi.org/10.1093/jxb/ers165

Mahan, J. R., & Yeater, K. M. (2008). Agricultural applications of a low-cost infrared thermometer. *Comput. Electron. Agric., 64*(2), 262-267. https://doi.org/10.1016/j.compag.2008.05.017

Martin, E. C., Stephens, W., Wiedenfeld, R., Bittenbender, H. C., Beasley Jr., J. P., Moore, J. M., ... Gallian, J. J. (2007). Sugar, oil, and fiber. In R. J. Lascano & R. E. Sojka (Eds.), *Irrigation of agricultural crops* (pp. 279-335). Agronomy Monograph 30. Madison, WI: ASA. https://doi.org/10.2134/agronmonogr30.2ed.c9

Melvin, S. R., & Yonts, C. D. (2009). Irrigation scheduling: Checkbook method. EC709. Lincoln, NE: University of Nebraska Extension. Retrieved from http://extensionpublications.unl.edu/assets/pdf/ec709.pdf

Möller, M., Alchanatis, V., Cohen, Y., Meron, M., Tsipris, J., Naor, A., ... Cohen, S. (2007). Use of thermal and visible imagery for estimating crop water status of irrigated grapevine. *J. Exp. Bot., 58*(4), 827-838. https://doi.org/10.1093/jxb/erl115

Moriasi, D. N., Arnold, J. G., Van Liew, M. W., Bingner, R. L., Harmel, R. D., & Veith, T. L. (2007). Model evaluation guidelines for systematic quantification of accuracy in watershed simulations. *Trans. ASABE, 50*(3), 885-900. https://doi.org/10.13031/2013.23153

Muñoz-Carpena, R. (2004). Field devices for monitoring soil water content. Bulletin 343. Gainesville, FL: University of Florida Institute of Food and Agricultural Sciences. Retrieved from https://edis.ifas.ufl.edu/ae266

Nash, J. E., & Sutcliffe, J. V. (1970). River flow forecasting through conceptual models: Part I. A discussion of principles. *J. Hydrol., 10*(3), 282-290. https://doi.org/10.1016/0022-1694(70)90255-6

Nayak, S. S. (2005). Thermal imagery and spectral reflectance based system to monitor crop condition. MS thesis. Lubbock, TX: Texas Tech University, Department of Mechanical Engineering.

Nordstokke, D. W., & Zumbo, B. D. (2010). A new nonparametric Levene test for equal variances. *Psicologica, 31*(2), 401-430.

Nordstokke, D. W., Zumbo, B. D., Cairns, S. L., & Saklofske, D. H. (2011). The operating characteristics of the nonparametric Levene test for equal variances with assessment and evaluation data. *Pract. Assess. Res. Eval., 16*(5). Retrieved from https://scholarworks.umass.edu/pare/vol16/iss1/5/

O'Shaughnessy, S. A., Evett, S. R., Colaizzi, P. D., & Howell, T. A. (2011). Using radiation thermography and thermometry to evaluate crop water stress in soybean and cotton. *Agric. Water Mgmt., 98*(10), 1523-1535. https://doi.org/10.1016/j.agwat.2011.05.005

O'Toole, J. C., & Real, J. G. (1986). Estimation of aerodynamic and crop resistances from canopy temperature. *Agron. J., 78*(2), 305-310. https://doi.org/10.2134/agronj1986.00021962007800020019x

Payero, J. O., & Irmak, S. (2006). Variable upper and lower crop water stress index baselines for corn and soybean. *Irrig. Sci., 25*(1), 21-32. https://doi.org/10.1007/s00271-006-0031-2

Pou, A., Diago, M. P., Medrano, H., Baluja, J., & Tardaguila, J. (2014). Validation of thermal indices for water status identification in grapevine. *Agric. Water Mgmt., 134*, 60-72. https://doi.org/10.1016/j.agwat.2013.11.010

Raschke, K. (1960). Heat transfer between the plant and the environment. *Ann. Rev. Plant Physiol., 11*(1), 111-126. https://doi.org/10.1146/annurev.pp.11.060160.000551

Sadler, E. J., Camp, C. R., Evans, D. E., & Millen, J. A. (2002). Corn canopy temperatures measured with a moving infrared thermometer array. *Trans. ASAE, 45*(3), 581-591. https://doi.org/10.13031/2013.8855

Sepaskhah, A. R., Nazemsadat, S. M. J., & Kamgarhaghighi, A. A. (1988). Estimation of upper limit canopy to air temperature differential for sugarbeet using indirect measurement of turgor potential. *Iran Agric. Res., 7*(2), 107-122.

Sharma, V., Nicholson, C., Bergantino, T., Cowley, J., Hess, B., & Tanaka, J. (2018). Wyoming Agricultural Climate Network (WACNet). Laramie, WY: University of Wyoming. Retrieved from http://www.wyagresearch.org/research/fdb/2018-off-wyoming-agricultural-climate-network.pdf

Shellie, K. C. (2006). Vine and berry response of Merlot (*Vitis vinifera* L.) to differential water stress. *American J. Enol. Vitic., 57*(4), 514-518.

Tanner, C. B. (1963). Plant temperatures. *Agron. J., 55*(2), 210-211. https://doi.org/10.2134/agronj1963.00021962005500020043x

Trajkovic, S., Todorovic, B., & Stankovic, M. (2003). Forecasting of reference evapotranspiration by artificial neural networks. *J. Irrig. Drain. Eng., 129*(6), 454-457. https://doi.org/10.1061/(ASCE)0733-9437(2003)129:6(454)

USDA. (1998). Soil survey of Jerome and part of Twin Falls County, Idaho. Washington, DC: USDA Natural Resources Conservation Service. Retrieved from www.nrcs.usda.gov/wps/portal/nrcs/surveylist/soils/survey/state/?stateId=ID

USDA. (2019). USDA web soil survey. Washington, DC: USDA Natural Resources Conservation Service. Retrieved from https://websoilsurvey.nrcs.usda.gov/app/

van Zyl, J. L. (1987). Diurnal variation in grapevine water stress as a function of changing soil water status and meteorological conditions. *South African J. Enol. Vitic., 8*(2), 8. https://doi.org/10.21548/8-2-2314

Vellidis, G., Tucker, M., Perry, C., Kvien, C., & Bednarz, C. (2008). A real-time wireless smart sensor array for scheduling irrigation. *Comput. Electron. Agric., 61*(1), 44-50. https://doi.org/10.1016/j.compag.2007.05.009

Werner, H. (1993). Checkbook irrigation scheduling: Irrigation management manual for South Dakota. EC897. Brookings, SD: South Dakota State Extension. Retrieved from https://openprairie.sdstate.edu/cgi/viewcontent.cgi?article=1460&context=extension_circ

Williams, L. E. (2014). Determination of evapotranspiration and crop coefficients for a chardonnay vineyard located in a cool climate. *American J. Enol. Vitic., 65*(2), 159-169. https://doi.org/10.5344/ajev.2014.12104

Williams, L. E., & Baeza, P. (2007). Relationships among ambient temperature and vapor pressure deficit and leaf and stem water potentials of fully irrigated, field-grown grapevines. *American J. Enol. Vitic., 58*(2), 173-181.

Williams, L. E., & Trout, T. J. (2005). Relationships among vine- and soil-based measures of water status in a Thompson seedless vineyard in response to high-frequency drip irrigation. *American J. Enol. Vitic., 56*(4), 357-366.

Wright, J. L. (1982). New evapotranspiration crop coefficients. *J. Irrig. Drain., 108*(IR2), 57-74.

Yapo, P. O., Gupta, H. V., & Sorooshian, S. (1996). Automatic calibration of conceptual rainfall-runoff models: Sensitivity to calibration data. *J. Hydrol., 181*(1), 23-48. https://doi.org/10.1016/0022-1694(95)02918-4

Zotarelli, L., Dukes, M. D., & Paranhos, M. (2013). Minimum number of soil moisture sensors for monitoring and irrigation purposes. HS1222. Gainesville, FL: University of Florida Institute of Food and Agricultural Sciences. Retrieved from https://edis.ifas.ufl.edu/hs1222